Selective CO_2 Capture in Metal-Organic Frameworks with Azine-Functionalized Pores Generated by Mechanosynthesis

Mohammad Yaser Masoomi,[†,^] Kyriakos C. Stylianou,[‡,^] Ali Morsali,[†*] Pascal Retailleau[§] and Daniel Maspoch[‡¤*]

[†]Department of Chemistry, Faculty of Sciences, Tarbiat Modares University, P.O. Box 14115-175, Tehran, Islamic Republic of Iran

[‡] ICN2 – Institut Catala de Nanociencia i Nanotecnologia, Campus UAB, 08193 Bellaterra (Barcelona), Spain

[§] Service de Cristallochimie, Institut de Chimie des Substances Naturelles-CNRS, Bât 27, 1 Avenue de la Terrasse, 91190 Gif sur Yvette, France

[¤] Institució Catalana de Recerca i Estudis Avançats (ICREA), 08100 Barcelona, Spain

^ Contributed equally to this work

Supporting Information Placeholder

ABSTRACT: Two new 3D, porous Zn(II)-based metal-organic frameworks, containing azine-functionalized pores, have been readily and quickly isolated via mechanosynthesis, by using a non-linear dicarboxylate and linear N-donor ligands. The use of non-functionalized and methyl-functionalized N-donor ligands has led to the formation of frameworks with different topology, metal-ligand connectivities, and therefore with different pore sizes and accessible volumes. Despite this, both MOFs possess comparable BET surface areas and CO_2 uptakes at 273 and 298 K at 1 bar. The network with narrow and interconnected pores in three dimensions show greater affinity for CO_2 compared to the network with 1D and relatively large pores – attributable to the more effective interactions with the azine groups.

Combustion of fossil fuels results in emission of CO_2 into the atmosphere, which is now known to cause severe global climatic and environmental changes.[1,2] One strategy to mitigate these effects is to optimize selective CO_2 capture and storage by developing new adsorbents with high storage capacity and adsorption selectivity for CO_2.[3-5] Porous metal-organic frameworks (MOFs) assembled from metal ions and organic linkers have recently begun to be explored as a potential new class of CO_2 adsorbents, owing to their very high surface areas, tunable pore sizes and shapes, adjustable pore surface functionality, and flexible structures.[6-8] Tuning of the chemical functionalities of the pore walls in MOFs should help to increase CO_2 uptake and adsorption selectivity.[9,10] This can be accomplished by functionalizing the pores with either of two groups: coordinatively unsaturated metal ions[11,12]; or Lewis basic groups (*e.g.* amine[13-17] and hydroxyl[18] groups).

Herein we report that the control of the pore size of MOFs functionalized with azine groups enables greater interactions between the host framework and guest CO_2 molecules.[19] Our strategy relies on pillaring 2D layers comprising Zn(II) ions and the V-shaped dicarboxylate ligand 4,4′-oxybisbenzoic acid (H_2oba), with linear pyridyl-based ligands.[20-22] The selected pillaring ligands are 1,4-bis(4-pyridyl)-2,3-diaza-1,3-butadiene (4-bpdb) and 2,5-bis(4-pyridyl)-3,4-diaza-2,4-hexadiene (4-bpdh), which lead to $[Zn_2(oba)_2(4\text{-bpdb})]\cdot(DMF)_x$ (**TMU-4: TMU** stands for **T**arbiat **M**odares **U**niversity) and $[Zn_2(oba)_2(4\text{-bpdh})]\cdot(DMF)_y$ (**TMU-5**), respectively.[23] Considering that the pores of MOFs constructed from layers pillared by linear ligands are usually delimited by these ligands[24], and that the selected ligands contain a bridging azine group in the middle (Scheme 1), we hypothesized -and subsequently confirmed- that the pores of the MOFs should contain two internal Lewis basic sites per ligand. **TMU-4** shows 1D (Fig. 1), relatively large pores (size: 6.8 x 7.8 Å, including van der Waals radii), whereas **TMU-5** shows 3D, interconnected, narrow pores (Fig. 2) (size: 5.6 x 3.8 Å, including van der Waals radii). We observed that the combination of pore size (narrow and interconnected) and pore functionalization (azine groups) favor the host-guest (CO_2) interactions.[25] Interestingly, both MOFs were synthesized easily and rapidly via mechanosynthesis.[26-35] Macroscale crystals of each MOF, suitable for single-crystal X-ray diffraction, were prepared by heating a mixture of $Zn(NO_3)_2\cdot6(H_2O)$, H_2oba and either 4-bpdb or 4-bpdh, in DMF at 80 °C for 72 hours.

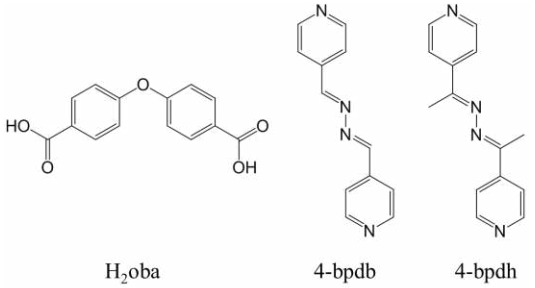

H_2oba 4-bpdb 4-bpdh

Scheme 1. Chemical structure of H_2oba, 4-bpdb and 4-bpdh. Note the bridging azine group at the center of 4-bpdb and 4-bpdh.

Framework **TMU-4** was prepared by mechanosynthesis (grinding by hand) of a mixture of $Zn(OAc)_2\cdot2H_2O$, H_2oba and 4-bpdb for 15 minutes. The resulting powder was washed once with a small amount of DMF to remove any traces of unreacted organic ligands or/and metal salts, and then dried in air to afford a yellow crystalline powder (yield: 85%).[36] The simulated (derived from the single crystal structure of **TMU-4**) and experimental (resulting from the mechanosynthesized powder) powder X-ray diffraction (PXRD) patterns are consistent (Figure S3 in the SI), confirming

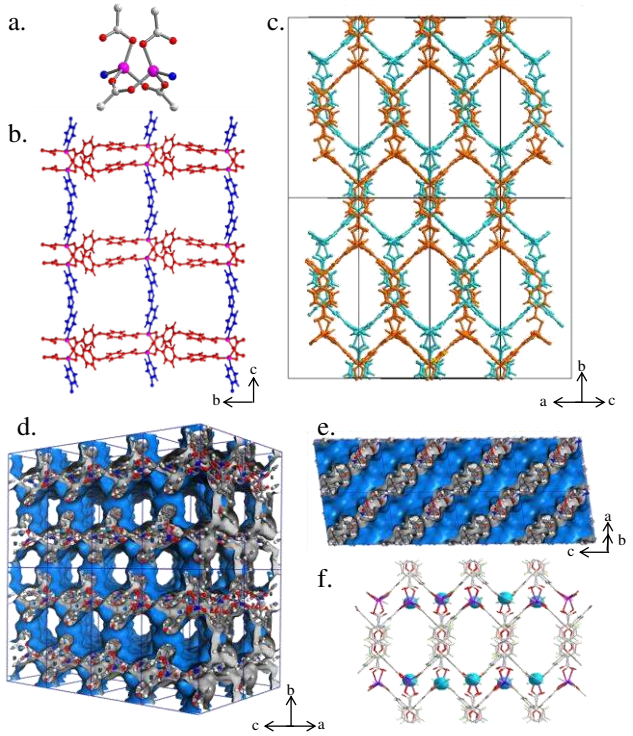

Figure 1. (a) Ball and stick representation of the binuclear Zn_2 unit (O: red; N: blue; C: grey; and Zn: pink). **(b)** Layers of Zn(II)-oba (in red) pillared by 4-bpdb (in blue). **(c)** The packing of the structure leads to a doubly interpenetrated (in orange and cyan) framework possessing 1D pores, **(d)** and **(e)** 3D Connolly surface representation of porous **TMU-4** along [1 0 1] direction and that the channels formed are one dimensional respectively, and **(f)** Representation of the pores highlighting the azine groups (sky blue balls) pointing towards the pores of **TMU-4.** In the Connolly surface representations, gray represents outside the surface and blue, inside the surface.

that the mechanosynthesized **TMU-4** is structurally identical to **TMU-4** prepared through conventional heating, and that it can be obtained as a pure phase (as also evidenced by elemental analysis; see SI). **TMU-4** is based on a binuclear Zn_2 unit (Zn#1 and Zn#2), in which both tetrahedral Zn(II) centers are coordinated to three carboxylate O atoms (for Zn#1: O1, O4, O10, and for Zn#2: O5, O6, O9) from three fully deprotonated oba ligands, and one N atom (Zn#1: N1 and Zn#2: N4) from the 4-bpdb ligand (Figure 1a). The distance between Zn#1 and Zn#2 is 3.441 Å. Each non-linear (angle: 125.12º) dicarboxylate oba ligand binds three consecutive Zn(II) centers from two different Zn_2 units, thereby forming 2D sheets (Fig. 1b and S1 in the SI). The coordination modes of a single oba ligand within **TMU-4** differ according to the carboxylate functional group: one of the carboxylate groups is bidentate and bridges both Zn#1 and Zn#2 centers of the unit in a *syn-syn* mode (mean distance: 1.994 Å), whereas the other one is monodentate and binds to either Zn#1 or Zn#2 (distance: 1.939 Å). The 2D sheets are connected through the linear 4-bpdb, extending the structure in three dimensions. Although **TMU-4** is doubly interpenetrated, it still possesses large 1D pore channels (size: 6.8 x 7.8 Å; 40% void space per unit cell)[37] running along the [1 0 1] direction (Fig. 1c-e). As shown in Fig. 1f, the internal surface of these pores is functionalized with the azine groups (shown in sky blue) of the 4-bpdb ligands.

TMU-5 was prepared using the same mechanochemical conditions as for **TMU-4**, but instead of 4-bpdb, we used 4-bpdh (yield: 80%). Interestingly, the simple introduction of two methyl groups in the N-donor pillar ligand induced the formation of a different structure to that of **TMU-4**: **TMU-5** is based on a binuclear pad-

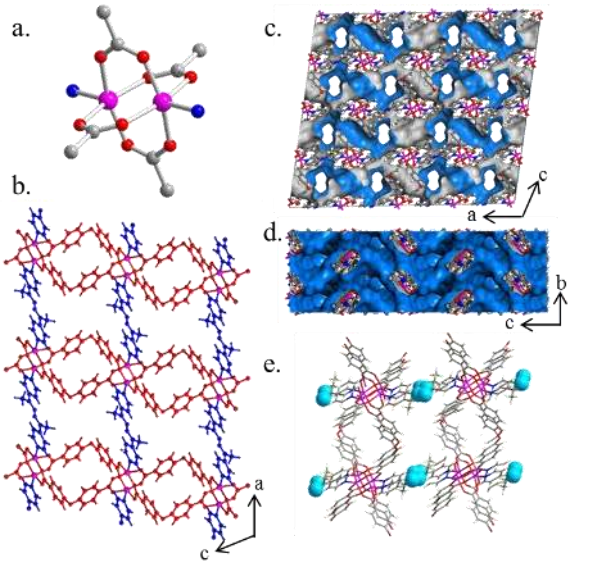

Figure 2. (a) Representation of the Zn_2 paddlewheel unit within **TMU-5**. **(b)** Layers of Zn(II)-oba (in red) pillared by 4-bpdh (in blue). **(c)** and **(d)** Connolly surface representation along *b*- and *a*-axis respectively, showing that **TMU-5** is porous and comprises interconnected pores. **(e)** Representation of the pores, highlighting the azine groups (in sky blue). Color code: O: red; N: blue; C: grey; and Zn: pink. Connolly surface: gray represents outside the surface and blue, inside the surface.

dlewheel Zn(II) unit (Fig. 2a), in which four carboxylate O atoms from four adjacent oba ligands form an approximate equatorial square plane (Zn–O carboxylate distances: 2.025 to 2.054 Å). The coordination environment of each Zn(II) center is completed by one N atom from 4-bpdh in the axial position (mean distance: 2.033Å). The separation of the Zn(II) centers within the paddlewheel unit is 2.937 Å, meaning that the Zn(II) ions are closer together than in **TMU-4**. As in **TMU-4**, the orientation of the oba ligands (angle: 120.70°) around the paddle-wheel Zn(II) units leads to the formation of 2D layers pillared by 4-bpdh ligands to yield a 3D framework (Fig. 2b and S2 in the SI). **TMU-5** possess narrower channels than those in **TMU-4** (size: 5.6 x 3.8 Å; 34% void space per unit cell)[37] running along the *b*-axis; however, these are interconnected along the three dimensions (Figures 1c-d), due to the large separation (distance: 8.192 Å) of the neighboring (oba or 4-bpdh) ligands. As seen in Fig. 2e, these channels are also functionalized with azine groups (shown in sky blue).

Thermogravimetric analysis (TGA) of **TMU-4** and **TMU-5** revealed a first weight loss in the temperature range of 100-315 ºC (15.9 %) and 100-290 ºC (16.1 %), respectively, attributed to the loss of guest DMF molecules adsorbed during the washing step. Then, a second weight loss was observed in the range of 315-500 ºC for **TMU-4** and 290-500 ºC for **TMU-5**, corresponding to the decomposition of the frameworks (Figure S6 in the SI). These observations confirmed that the pores of the mechanosynthesized **TMU-4** and **TMU-5** were available for the adsorption of DMF molecules. This result is similar with what is found for the corresponding **TMU-4** and **TMU-5** synthesized by conventional heating, for which TGA showed additional weight losses of 16.5% (100-315 ºC) in **TMU-4** and 18% (100-290ºC) in **TMU-5** (Fig. S6 in the SI), both of which we ascribed to the removal of guest DMF molecules. We also investigated the stability of both frameworks in H_2O for 24 h at room temperature. In both cases, a new crystalline phase was formed as confirmed by PXRD (Fig. S5 in the SI). Single crystal X-ray diffraction experiments were not successful due to the poor quality of the crystals after being exposed in H_2O.[17]

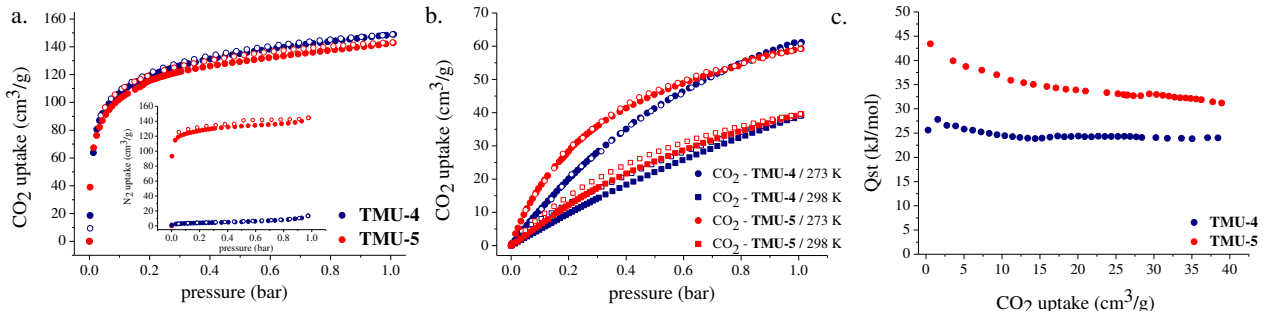

Figure 3. (a) Type I CO_2 isotherms at 195 K and 1 bar collected on mechanosynthesized **TMU-4** and **TMU-5** after activating each one at 40 ºC overnight under vacuum. Inset shows N_2 isotherms. (b) CO_2 isotherms collected at 273 K and 298 K**. (c)** Isosteric heat of adsorption *(Q_{st})* for CO_2 at different CO_2 loadings.

A type II N_2 isotherm collected at 77 K and 1 bar on the mechanochemically synthesized **TMU-4** (after activation at 40 ºC) revealed that N_2 molecules couldn't diffuse within its pores under these conditions. Interestingly, **TMU-4** is porous to CO_2 at 195 K and 1 bar (148.90 cm^3/g at 1 bar; BET surface area calculated over p/p^0 = 0.02-0.3: 517.9 m^2/g) (Fig. 3a). The pore volume calculated from the CO_2 adsorption is 0.298 cm^3/g (compared to 0.367 cm^3/g in the rigid host structure). **TMU-4** shows a pore size of 6.8 x 7.8 Å, large enough to be, in principle, accessible for both N_2 and CO_2 (kinetic diameters for CO_2: 3.30 Å and N_2: 3.75 Å) adsorption. We reasoned that this selectivity could be partially explained by the existence of structural changes during gas adsorption, the existence of structural defects and/or the surface functionalization and consequently to the interactions between the CO_2 molecule and the electron-donating, uncoordinated nitrogen atoms of the azine groups decorating the pores.

Surprisingly, even though **TMU-5** has narrower pores than **TMU-4**, we found that it is porous to both CO_2 (142.88 cm^3/g at 1 bar; BET surface area: 502.7 m^2/g) at 195 K and N_2 (144.49 cm^3/g at 1 bar; BET surface area: 400.8 m^2/g) at 77 K, for which it showed reversible type-I isotherms (Fig. 3a).[38] The pore volumes for **TMU-5**, derived from the CO_2 and N_2 adsorption branches, were found to be 0.286 cm^3/g and 0.227 cm^3/g, respectively (compared to 0.235 cm^3/g in the static structure). These results suggest that N_2 can almost fill the pores of **TMU-5**, whereas (polar) CO_2 can fill the pores and at the same time induce structural re-arrangements that expand the pores and consequently, the structural architecture. Similar behavior has been recently described in other MOFs: the adsorption of bulky xylene molecules within a flexible framework induced structural changes.[39] PXRD study after the sorption studies revealed that both **TMU-4** and **TMU-5** are robust (Fig. S8 in the SI).

The sorption behavior of **TMU-4** and **TMU-5** towards CO_2 and N_2 led us to investigate their respective CO_2/N_2 selectivities at 298 K based on the ratio of single-component uptakes and using the IAST model for the equimolar gas mixture.[40] The calculated CO_2/N_2 selectivity for **TMU-5** (32:1) is slightly greater than that of **TMU-4** (28:1) (ratio of single-component uptakes). The selectivity of the equimolar mixture of CO_2 and N_2 was also estimated using IAST calculations. It was found a similar tendency for both frameworks, with selectivity values of 20.9 for **MTU-4** and 25.2 for **TMU-5.** These selectivity values gradually decrease from 25.2 to 23.2 and from 20.9 to 18.4 at 1 bar for **TMU-5** and **TMU-4**, respectively (Fig. S9-10 in the SI). These are moderate values for MOFs, lower than that of $Zn_2(TCBP)(DMF)_2$, which is found to be ~45.[41]

To assess the strength of interactions between CO_2 and each host framework, we also collected CO_2 isotherms at 273 K at 1 bar. The CO_2 isotherms for both frameworks show reversible type I behavior (Fig. 3b). At 273 K and 1 bar, **TMU-4** and **TMU-5** adsorbed 61.16 and 59.15 cm^3/g of CO_2, respectively. A comparable uptake at 1 bar was also observed at 298 K from both frameworks (Figure 2b). However, an important feature derived from these isotherms is that at low pressure, **TMU-5** adsorbed higher amounts of CO_2 than **TMU-4**. For example, at 273 K and 0.25 bar **TMU-5** adsorbed 32.71 cm^3/g, whereas **TMU-4** adsorbed 24.39 cm^3/g. This observation reveals that the interactions between the azine groups pointing towards the narrow pores of **TMU-5** and CO_2 are more pronounced than those in **TMU-4**. The isosteric heat of adsorption *(Q_{st})* was calculated using the Clausius-Clapeyron equation[42] using the adsorption branches of the isotherms measured at 273 and 298 K in order to check how the pore functionalization and size can influence the affinity of **TMU-4** and **TMU-5** for CO_2. The Q_{st} of **TMU-5** for CO_2 was 43.4 kJ/mol at zero coverage - a much higher value than that for **TMU-4** (25.6-27.8 kJ/mol) (Fig. 3c). This observation confirms that the narrow and interconnected pores functionalized with azine groups of **TMU-5** generates greater interactions with CO_2 compared with the interactions occurred within the large 1D pores in **TMU-4**, which are functionalized with azine groups.[20,43] It is also in correlation with the fact that azine groups of **TMU-5** are more electron-rich than those of **TMU-4**.[38] As seen in Fig. 3c, the strength of interactions of **TMU-4** and **TMU-5** with CO_2 at high loadings are gradually decreased.

To conclude, the mechanochemical grinding of N-donor ligands with Zn(II) and H_2oba resulted in the formation of two frameworks – **TMU-4** and **TMU-5** possessing different structural topologies, metal-ligand connectivities and therefore different pore sizes. Despite this, the pore surface in both networks is azine decorated available for the CO_2 capture. Detailed sorption studies revealed that both MOFs introduce moderately strong interactions with CO_2, which are more pronounced within **TMU-5** (narrow pores). This study demonstrates that the size of the azine functionalized pores are key factors for the capture of CO_2 and since both frameworks can be obtained within only 15 minutes via mechanosynthesis, can be therefore used for industrial studies on CO_2 capture.

ASSOCIATED CONTENT

Supporting Information

Detailed synthetic procedures for the isolation of **TMU-4** and **TMU-5**, additional graphs determining their structure, PXRD patterns and TGA profiles are provided. The supplementary crystallographic data were deposited with the Cambridge Crystallographic Data Centre (CCDC) as entry CCDC 973905 and 973906. This material is available free of charge via the Internet at http://pubs.acs.org.

AUTHOR INFORMATION

Corresponding Author

E-mail: morsali_a@modares.ac.ir and daniel.maspoch@icn.cat

Notes

The authors declare no competing financial interest.

ACKNOWLEDGMENT

This work is supported by Tarbiat Modares University and by MINECO-Spain, under projects MAT2012-30994 and CTQ2011-16009-E. KCS grateful acknowledges EU for the Marie Curie Fellowship (300390 NanoBioMOFs FP7-PEOPLE-2011-IEF).

REFERENCES

(1) Petit, J. R.; Jouzel, J.; Raynaud, D.; Barkov, N. I.; Barnola, J. M.; Basile, I.; Bender, M.; Chappellaz, J.; Davis, M.; Delaygue, G.; Delmotte, M.; Kotlyakov, V. M.; Legrand, M.; Lipenkov, V. Y.; Lorius, C.; Pepin, L.; Ritz, C.; Saltzman, E.; Stievenard, M. *Nature* 1999, 399, 429.

(2) http://www.iea.org/.

(3) Ahmed, A.; Forster, M.; Clowes, R.; Bradshaw, D.; Myers, P.; Zhang, H. *J. Mater. Chem. A* 2013, 1, 3276.

(4) Yang, S.; Sun, J.; Ramirez-Cuesta, A. J.; Callear, S. K.; David, W. I. F.; Anderson, D. P.; Newby, R.; Blake, A. J.; Parker, J. E.; Tang, C. C.; Schroeder, M. *Nat. Chem.* 2012, 4, 887.

(5) Wu, H.; Reali, R. S.; Smith, D. A.; Trachtenberg, M. C.; Li, J. *Chem. Eur. J.* 2010, 16, 13951.

(6) An, J.; Farha, O. K.; Hupp, J. T.; Pohl, E.; Yeh, J. I.; Rosi, N. L. *Nat. Commun.* 2012, 3.

(7) D'Alessandro, D. M.; Smit, B.; Long, J. R. *Angew. Chem. Int. Ed.* 2010, 49, 6058.

(8) Zhang, Z.; Zhao, Y.; Gong, Q.; Li, Z.; Li, J. *Chem. Commun.* 2013, 49, 653.

(9) Sumida, K.; Rogow, D. L.; Mason, J. A.; McDonald, T. M.; Bloch, E. D.; Herm, Z. R.; Bae, T.-H.; Long, J. R. *Chem. Rev.* 2012, 112, 724.

(10) Li, T.; Chen, D.-L.; Sullivan, J. E.; Kozlowski, M. T.; Johnson, J. K.; Rosi, N. L. *Chem. Sci*. 2013, 4, 1746.

(11) Angamuthu, R.; Byers, P.; Lutz, M.; Spek, A. L.; Bouwman, E. *Science* 2010, 327, 313.

(12) Xue, D. X.; Cairns, A. J.; Belmabkhout, Y.; Wojtas, L.; Liu, Y. L.; Alkordi, M. H.; Eddaoudi, M. *J. Am. Chem. Soc.* 2013, 135, 7660.

(13) Vaidhyanathan, R.; Iremonger, S. S.; Shimizu, G. K. H.; Boyd, P. G.; Alavi, S.; Woo, T. K. *Science* 2010, 330, 650.

(14) Stylianou, K. C.; Warren, J. E.; Chong, S. Y.; Rabone, J.; Bacsa, J.; Bradshaw, D.; Rosseinsky, M. J. *Chem. Commun.* 2011, 47, 3389.

(15) McDonald, T. M.; Lee, W. R.; Mason, J. A.; Wiers, B. M.; Hong, C. S.; Long, J. R. *J. Am. Chem. Soc.* 2012, 134, 7056.

(16) An, J.; Geib, S. J.; Rosi, N. L. *J. Am. Chem. Soc.* 2010, 132, 38.

(17) Yuan, B.; Ma, D.; Wang, X.; Li, Z.; Li, Y.; Liu, H.; He, D. *Chem. Commun.* 2012, 48, 1135.

(18) Corma, A.; Garcia, H.; Llabres i Xamena, F. X. L. I. *Chem. Rev.* 2010, 110, 4606.

(19) Demessence, A.; D'Alessandro, D. M.; Foo, M. L.; Long, J. R. *J. Am. Chem. Soc.* 2009, 131, 8784.

(20) Gao, W.-Y.; Yan, W.; Cai, R.; Williams, K.; Salas, A.; Wojtas, L.; Shi, X.; Ma, S. *Chem. Commun.* 2012, 48, 8898.

(21) Lan, A.; Li, K.; Wu, H.; Olson, D. H.; Emge, T. J.; Ki, W.; Hong, M.; Li, J. *Angew. Chem. Int. Ed.* 2009, 48, 2334.

(22) Pramanik, S.; Zheng, C.; Zhang, X.; Emge, T. J.; Li, J. *J. Am. Chem. Soc.* 2011, 133, 4153.

(23) For mechanosynthesized **TMU-4** and **TMU-5***:* x = y = 0. Using conventional heating reaction: x = 2 and y = 2.

(24) Vaidhyanathan, R.; Bradshaw, D.; Rebilly, J. N.; Barrio, J. P.; Gould, J. A.; Berry, N. G.; Rosseinsky, M. J. *Angew. Chem. Int. Ed.* 2006, 45, 6495.

(25) Li, J. R.; Ma, Y. G.; McCarthy, M. C.; Sculley, J.; Yu, J. M.; Jeong, H. K.; Balbuena, P. B.; Zhou, H. C. *Coord. Chem. Rev.* 2011, 255, 1791.

(26) Gassensmith, J. J.; Furukawa, H.; Smaldone, R. A.; Forgan, R. S.; Botros, Y. Y.; Yaghi, O. M.; Stoddart, J. F. *J. Am. Chem. Soc.* 2011, 133, 15312.

(27) Ramsahye, N. A.; Maurin, G.; Bourrelly, S.; Llewellyn, P. L.; Devic, T.; Serre, C.; Loiseau, T.; Ferey, G. Adsorption-Journal of the International Adsorption Society 2007, 13, 461.

(28) Yuan, W.; Friščić, T.; Apperley, D.; James, S. L. *Angew. Chem. Int. Ed.* 2010, 49, 3916.

(29) Friscic, T.; Fabian, L. Cryst. Eng. Comm. 2009, 11, 743.

(30) Fujii, K.; Garay, A. L.; Hill, J.; Sbircea, E.; Pan, Z.; Xu, M.; Apperley, D. C.; James, S. L.; Harris, K. D. M. *Chem. Commun.* 2010, 46, 7572.

(31) Beldon, P. J.; Fábián, L.; Stein, R. S.; Thirumurugan, A.; Cheetham, A. K.; Friščić, T. *Angew. Chem. Int. Ed.* 2010, 49, 9640.

(32) Friščić, T.; Reid, D. G.; Halasz, I.; Stein, R. S.; Dinnebier, R. E.; Duer, M. J. *Angew. Chem. Int. Ed.* 2010, 49, 712.

(33) Cliffe, M. J.; Mottillo, C.; Stein, R. S.; Bucar, D.-K.; Friscic, T. *Chem. Sci.* 2012, 3, 2495.

(34) Friscic, T. *Chem. Soc. Rev.* 2012, 41, 3493.

(35) Bennett, T. D.; Cao, S.; Tan, J. C.; Keen, D. A.; Bithell, E. G.; Beldon, P. J.; Friscic, T.; Cheetham, A. K. *J. Am. Chem. Soc.* 2011, 133, 14546.

(36) Yuan, W. B.; O'Connor, J.; James, S. L. *Cryst. Eng. Comm.* 2010, 12, 3515.

(37) Spek, A. L. Journal of Applied Crystallography 2003, 36, 7.

(38) Bhattacharya, B.; Haldar, R.; Dey, R.; Maji, T. K.; Ghoshal, D. *Dalton Trans.* 2014, 43, 2272.

(39) Stylianou, K. C.; Rabone, J.; Chong, S. Y.; Heck, R.; Armstrong, J.; Wiper, P. V.; Jelfs, K. E.; Zlatogorsky, S.; Bacsa, J.; McLennan, A. G.; Ireland, C. P.; Khimyak, Y. Z.; Thomas, K. M.; Bradshaw, D.; Rosseinsky, M. J. *J. Am. Chem. Soc.* 2012, 134, 20466.

(40) Nugent, P.; Belmabkhout, Y.; Burd, S. D.; Cairns, A. J.; Luebke, R.; Forrest, K.; Pham, T.; Ma, S.; Space, B.; Wojtas, L.; Eddaoudi, M.; Zaworotko, M. J. *Nature* 2013, 495, 80.

(41) Bae, Y.-S.; Farha, O. K.; Hupp, J. T.; Snurr, R. Q. *J. Mater. Chem.* 2009, 19, 2131.

(42) Dincă, M.; Long, J. R. *J. Am. Chem. Soc.* 2005, 127, 9376.

(43) Burd, S. D.; Ma, S.; Perman, J. A.; Sikora, B. J.; Snurr, R. Q.; Thallapally, P. K.; Tian, J.; Wojtas, L.; Zaworotko, M. J. *J. Am. Chem. Soc.* 2012, 134, 3663.

For Table of Contents Use Only

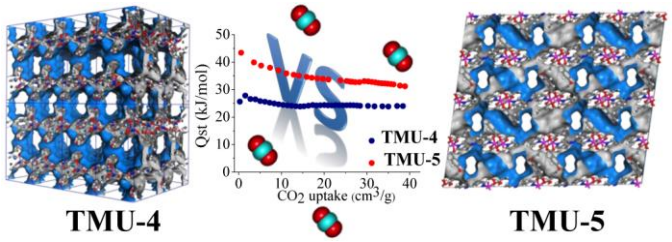

Two new 3D, porous Zn(II)-based MOFs, containing azine-functionalized pores, are mechanosynthesized by using dicarboxylate and N-donor ligands. The use of non- or methyl-functionalized N-donor ligands has led to the formation of frameworks with different topology, metal-ligand connectivities and therefore, different pore sizes and accessible volumes - having a direct impact on their sorption behavior and CO_2 capture.

Title: Selective CO_2 Capture in Metal-Organic Frameworks with Azine-Functionalized Pores Generated by Mechanosynthesis

Authors: Mohammad Yaser Masoomi, Kyriakos C. Stylianou, Ali Morsali, Pascal Retailleau and Daniel Maspoch